

# Long-term image storage and phase conjugation by a backward-stimulated echo in $\text{Pr}^{3+}:\text{LaF}_3$

M. K. Kim and R. Kachru

Molecular Physics Department, Chemical Physics Laboratory, SRI International, Menlo Park, California 94025

Received September 22, 1986; accepted December 4, 1986

We have observed spatial-image storage and phase conjugation, using a backward-stimulated echo in a solid sample. The image storage and the delayed phase conjugation were observed to last for at least 15 sec, which is  $3 \times 10^5$  times longer than the radiative lifetime of the excited state. The backward-stimulated echo produced on the  ${}^3H_4\text{-}{}^3P_0$  transition of  $\text{Pr}^{3+}:\text{LaF}_3$  is found to be a phase-conjugated spatial reproduction of the first excitation pulse. The image storage time depends strongly on the sample temperature.

The ability of stimulated echoes to store information in a single electronic state has recently become appreciated.<sup>1-5</sup> The backward-stimulated echo,<sup>1,2,4,6-10</sup> a stimulated-echo scheme using a counterpropagating excitation geometry, is especially useful for optical information storage because the echo can be spatially and temporally separated from the excitation pulses. The generation of a backward-stimulated echo in a solid sample was reported recently.<sup>8</sup> It has been known for some time that the stimulated-echo signal is a phase-conjugate replica of one of the excitation pulses.<sup>9</sup> The phase conjugation and spatial-image storage aspects of the stimulated echo were first demonstrated by Carlson *et al.*<sup>10</sup> in Yb vapor. Saari *et al.*<sup>11</sup> have demonstrated phase conjugation and image storage in a photochemically active octaethylporphyrin-doped polystyrene by photochemical hole burning.

We report the first demonstration to our knowledge of long-term spatial-information storage and phase conjugation for several seconds using the backward-stimulated echo in a solid sample. Specifically, we have observed the storage and retrieval of a two-dimensional spatial image inside a  $\text{Pr}^{3+}$ -doped  $\text{LaF}_3$  crystal at low temperature ( $<4.2$  K). Furthermore, we observe that the image recalled by the backward-stimulated echo is a phase-conjugate spatial replica of the first excitation pulse. We observe that the image storage lasts as long as 15 sec, which is  $3 \times 10^5$  times longer than the radiative lifetime of the excited state. The recording of the spatial images that we have observed requires rather a modest laser energy of  $10 \mu\text{J}$  per pulse. Although stimulated echo was previously observed to last as long as 30 min in a  $\text{Pr}^{3+}:\text{LaF}_3$  sample in the presence of strong magnetic field,<sup>3</sup> our observation is the first, to our knowledge, to demonstrate spatial-image storage and phase conjugation for a long time.

Phase conjugation and spatial-information storage by a stimulated echo are especially interesting because the information (both spatial and temporal) is stored during the interval between the second and the third pulses of the three-pulse excitation sequence required for echo generation. The spatial and temporal information is stored as the population modulation in the ground and excited states,

respectively, or in the phase memory of a nearly degenerate set of ground (or excited) levels.<sup>12,13</sup> At times longer than the radiative lifetime of the excited state, the information can be recalled by the third pulse from the ground state alone. Despite this ability to store information in the ground state, stimulated-echo storage time in vapor phase<sup>1,2,7</sup> is limited to a few microseconds because of the thermal motion of the atoms. This limitation does not apply to ions that produce a stimulated echo in a solid sample, and thus the technological implications of our results are evident.

Consider an assembly of ions in a crystal with a near-degenerate set of ground  $|0\rangle$  and excited  $|1\rangle$  states having a central transition frequency  $\omega_0$  and an inhomogeneous strain-broadened absorption linewidth  $\Delta\omega$  (full width at half-maximum). Let the ions be resonantly excited by three short laser pulses at time  $t_i$  ( $i = 1, 2, 3$ ). The laser electric field, assumed monochromatic for simplicity, is given by

$$E_i(\mathbf{r}) \exp[i(\mathbf{k}_i \cdot \mathbf{r} - \omega_0 t + \phi_i(\mathbf{r}))], \quad (1)$$

where  $E_i$  denotes the amplitude,  $\mathbf{k}_i$  denotes the wave vector, and  $\phi_i$  denotes an arbitrary phase factor of the  $i$ th excitation pulse. After the passage of the first two excitation pulses through the sample, the diagonal density matrix elements of any particular ion with absorption frequency  $\omega$  are given by

$$\rho_{00}(\mathbf{r}, t) = \sin^2 \frac{1}{2}[(\mathbf{k}_1 - \mathbf{k}_2) \cdot \mathbf{r} + (\phi_1 - \phi_2) - \Delta\omega t_{21}] \quad (2)$$

and  $\rho_{11} = 1 - \rho_{00}$ .

In Eq. (2),  $\Delta\omega = \omega - \omega_0$  and  $t_{ij} = t_i - t_j$ . In addition, for simplicity, it is assumed in Eq. (2) that  $\theta_1 = \theta_2 = \pi/2$ , where  $\theta_i = 2pE_i/\hbar\tau_i$  are the excitation pulse areas,  $p$  is the dipole transition moment, and  $\tau_i$  is the temporal pulse width. The backward-echo scheme is shown in Figs. 1(a) and 1(b). If, for simplicity, we assume that  $\theta = 0$  and substitute  $\mathbf{k}_2 = -\mathbf{k}_1$  and  $\mathbf{k}_1 = \mathbf{k}_2$  corresponding to Figs. 1(a) and (b), respectively, into Eq. (2), we see that the population distribution in the ground and excited states is modulated as a function of  $\Delta\omega$ , the detuning from the line center, after the passage of the second excitation pulse. The modulation frequency in the inhomogeneous line is the Fourier transform of the time-domain spectrum defined by the relative temporal separa-

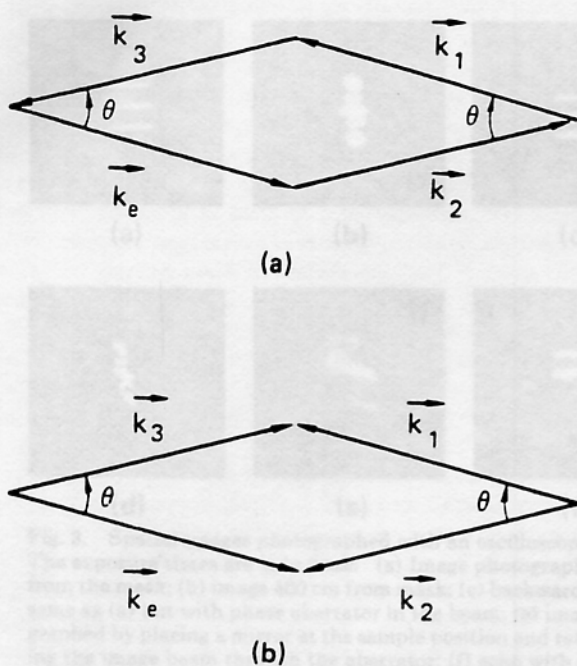


Fig. 1. Excitation schemes useful for backward-stimulated echo production in solids. Two of the several specific schemes are shown in (a) and (b).

tion between the excitation pulses. At pulse areas other than  $\pi/2$ , the modulation depth is reduced but the modulation frequency remains the same.

The excitation of the sample by the third pulse recalls the information stored in the ground and excited states, and the stimulated echo is generated at  $t = t_3 + t_{21}$ . The stimulated-echo amplitude  $E_e$ , which is proportional to  $\rho_{10}$ , is given by

$$E_e(\mathbf{r}, t) \propto \sin \theta_1(\mathbf{r}) \sin \theta_2(\mathbf{r}) \sin \theta_3(\mathbf{r}) \exp(-i\omega_0 t) \\ \times (\exp i\{(-\mathbf{k}_1 + \mathbf{k}_2 + \mathbf{k}_3) \cdot \mathbf{r} - \phi_1(\mathbf{r}) + \phi_2(\mathbf{r}) + \phi_3(\mathbf{r}) \\ - \Delta\omega[t - (t_3 + t_{21})]\} + \exp i\{(\mathbf{k}_1 - \mathbf{k}_2 + \mathbf{k}_3) \cdot \mathbf{r} \\ + \phi_1(\mathbf{r}) - \phi_2(\mathbf{r}) + \phi_3(\mathbf{r}) - \Delta\omega[t - (t_3 - t_{21})]\}). \quad (3)$$

In arriving at the above formula, we have implicitly neglect-

ed all relaxation mechanisms. Expression (3) shows that, for echo generation, the local microscopic dipole moment at any location in the sample has to rephase.<sup>12</sup> The rephasing condition means that the phases of all ions at any given location in the sample must be equal at the echo time. Furthermore, because the sample is longer than the wavelength, the echo generation also requires the phase-matching condition.<sup>12</sup> The phase-matching condition determines whether the dipoles along the entire sample radiate constructively to generate an echo.

Inspection of expression (3) shows that the first term always rephases, whereas the second one never does for solids. Thus the stimulated echo is always generated as long as the phase-matching condition is satisfied. Note that this is not the case for echo generation in the vapor phase, where the phase-matching condition is not independent of the rephasing condition.<sup>7,12</sup> Figure 1 shows two excitation schemes that we have used to generate backward-stimulated echo. Substituting the  $k$  vector relationships of Fig. 1(a) into expression (3) gives, for small pulse areas where  $\sin \theta_i \propto E_i$ ,

$$E_e(\mathbf{r}) \propto E_1(r)E_2(r)E_3(r)\exp i[-\omega_0 t + \mathbf{k}_e \cdot \mathbf{r} - \phi_1(\mathbf{r})], \quad (4)$$

where  $\mathbf{k}_e = -\mathbf{k}_1 + \mathbf{k}_2 + \mathbf{k}_3$ . Expression (4) demonstrates that the echo is phase conjugated with respect to the first pulse, regardless of the phases of the other excitation pulses. In the vapor phase the backward-generated echo is a phase conjugate with respect to the second excitation pulse.<sup>7-10,12</sup> It is also evident from expression (4) that, if the second and third excitation pulses are short (compared with  $T_2^*$ ) and the pulse area of the first pulse is small, the echo pulse is a phase-conjugate replica of the first pulse. If the first pulse consists of a whole series of pulses, the echo is again a replica of the first pulse<sup>4</sup>; i.e., it consists of a series of pulses in reverse temporal order. This latter scheme is one of several that are useful for an optical memory.

Another excitation scheme that produces a phase-matched backward echo is shown in Fig. 1(b). Here also the generated backward echo is a phase-conjugate replica of the first pulse. In fact, in solids the stimulated echo is always a phase conjugate with respect to the first pulse, in contrast to the vapor phase, where the forward and the backward echoes

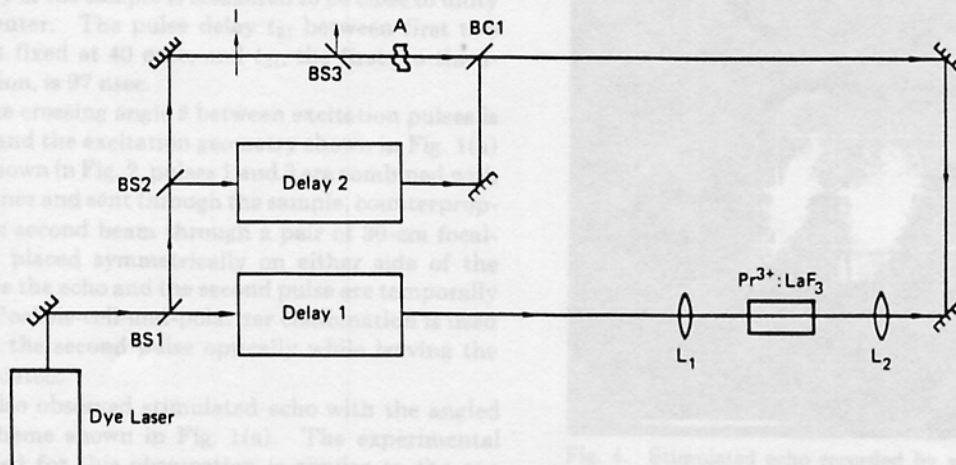


Fig. 2. Schematic of the experimental setup: BS1, BS2, and BS3 are beam splitters; BC is a beam combiner; L<sub>1</sub> and L<sub>2</sub> are 30-cm focal-length lenses; I is the image; A is a phase aberrator.



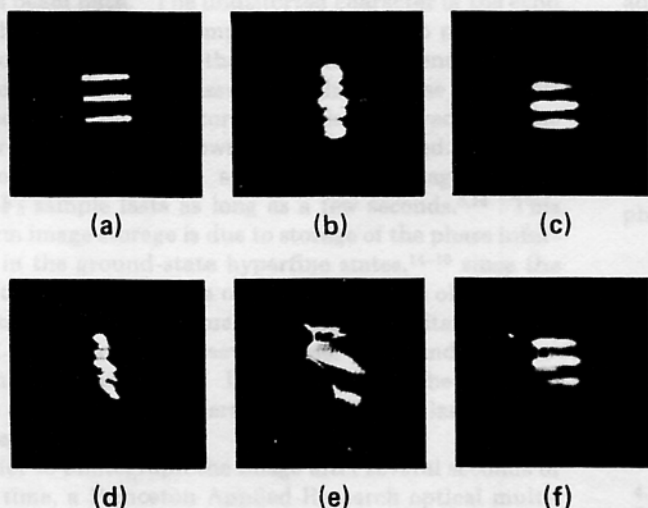


Fig. 3. Spatial images photographed with an oscilloscope camera. The exposure times are  $\frac{1}{8}$  to 2 sec. (a) Image photographed 30 cm from the mask; (b) image 400 cm from mask; (c) backward echo; (d) same as (a) but with phase aberrator in the beam; (e) image photographed by placing a mirror at the sample position and retroreflecting the image beam through the aberrator; (f) echo with the phase aberrator.

are phase conjugates with respect to the first and the second pulses, respectively.

A schematic of our experimental setup is shown in Fig. 2. A single YAG-laser-pumped dye laser operating at 10 Hz produces 5-nsec-long pulses with a spectral linewidth of 15 GHz. Usually the laser beam profile is far from Gaussian. The dye-laser pulses are resonant with the transition connecting the lowest Stark levels of the  $^3H_4$  ground and  $^3P_0$  excited levels ( $\lambda = 4778 \text{ \AA}$ ). Optical delay lines are used to delay the dye-laser pulse and form the second and third excitation pulses. The sample, consisting of 0.1% atomic concentration  $\text{Pr}^{3+}:\text{LaF}_3$  crystal, 12 mm long and 6 mm in diameter, is kept in a liquid-helium cryostat. The sample temperature can be varied between 4.2 and 1.2 K. The excitation pulses propagate along the crystal  $c$  axis and are linearly polarized so that the electric fields are normal to the  $c$  axis. The 3-mm-diameter excitation pulses have peak powers of 100 kW in the focal volume in the sample. The optical density of the sample is measured to be close to unity at the line center. The pulse delay  $t_{21}$  between first two pulses is kept fixed at 40 nsec, and  $t_{31}$ , the first- to third-pulse separation, is 97 nsec.

Initially, the crossing angle  $\theta$  between excitation pulses is kept at zero, and the excitation geometry shown in Fig. 1(a) is used. As shown in Fig. 2, pulses 1 and 3 are combined with a beam combiner and sent through the sample, counterpropagating to the second beam through a pair of 30-cm focal-length lenses placed symmetrically on either side of the sample. Since the echo and the second pulse are temporally separated, a Pockels-cell-and-polarizer combination is used to switch out the second pulse optically while leaving the echo unattenuated.

We have also observed stimulated echo with the angled excitation scheme shown in Fig. 1(a). The experimental apparatus used for this observation is similar to the one shown in Fig. 2, except that the pulses are angled with  $\theta = 10 \text{ mrad}$ . Because the pulses are angled, there are no excitation

pulses traveling along the propagation direction of the stimulated echo. The echo intensity for  $\theta = 10 \text{ mrad}$  is the same as for  $\theta = 0$ . This is consistent with the fact that, in a solid, the echo amplitude is undiminished as a function of  $\theta$ , as long as the excitation pulses are phase matched. This is to be contrasted with echo generation in the vapor phase, where the echo amplitude decreases exponentially with  $\theta$ , even when the phase-matching condition is satisfied. The minimum echo intensity is 0.5% of the excitation pulse intensity.

The spatial image to be stored and retrieved from the  $\text{Pr}^{3+}:\text{LaF}_3$  sample is carried by the first excitation pulse. The image, consisting of horizontal or vertical lines 0.35 mm wide on a transmission mask, is transferred to the first pulse by inserting the mask in the path of the beam. Figure 3(a) shows the image photographed with a Polaroid oscilloscope camera near the mask. Figure 3(b) shows the same image, photographed near the sample, which is 400 cm from the mask. The image shown in Fig. 3(b) appears distorted because of the far-field diffraction pattern from the object mask. The spatial image of the backward echo is obtained by inserting the beam splitter in the path of the first pulse, as shown in Fig. 2. The spatial image carried by the echo is shown in Fig. 3(c). The echo image is photographed at the same distance from the sample as the image mask. Figure 3(c) shows that the backward echo is a good reproduction of the image carried by the first pulse.

The phase-conjugate character of the echo is best demonstrated by placing a phase aberrator in the path of the image beam. As shown in Fig. 2, a phase aberrator consisting of a deformed piece of glass that changes the refractive index along the image wave front is placed in the path of the image-carrying excitation beam. Figure 3(d) shows the effect of the aberrator on the quality of the image, which is photographed near the sample, while Fig. 3(e) is obtained by placing a mirror at the sample to retroreflect back through the aberrator. In contrast to Fig. 3(b), the aberrated image is distorted near the sample. The presence of the phase aberrator in the path of the first pulse means that the echo pulse passes through it before being photographed. Figure

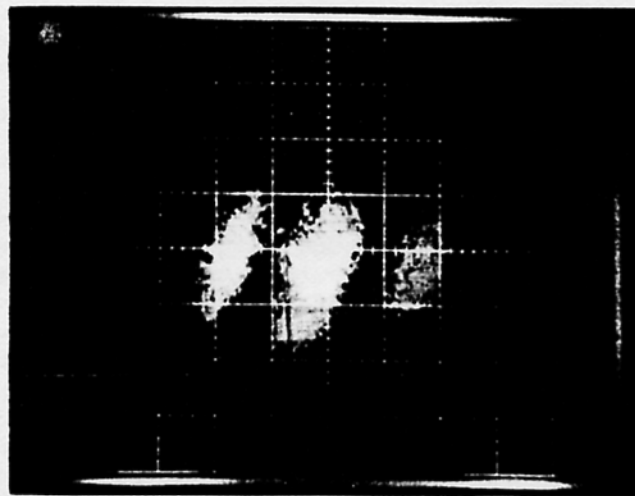


Fig. 4. Stimulated echo recorded by an OMA with  $t_{31} = 3 \text{ sec}$ . After the delay time the echo images are accumulated on the reticon array in the OMA for 2 sec and are subsequently displayed on the oscilloscope and photographed with a camera.

3(f) shows a spatial profile of the echo with the phase aberrator in its beam path. The undistorted character of the echo image shown in Fig. 3(f) implies that the echo produces a phase-conjugate replica of the first pulse and hence restores the distorted image as it passes through the phase aberrator. Phase-conjugate phase restoration is also observed when the backward-echo scheme shown in Fig. 1(b) is used.

We observe that the spatial-image storage in the  $\text{Pr}^{3+}:\text{LaF}_3$  sample lasts as long as a few seconds.<sup>8,14</sup> This long-term image storage is due to storage of the phase information in the ground-state hyperfine states,<sup>14-16</sup> since the  $^3P_0$  excited-state lifetime is only 50  $\mu\text{sec}$ .<sup>17</sup> To observe the image storage for a long time, we block the excitation pulse in front of the sample for several laser shots and then unblock only the third phase. In this way  $t_{31}$  can be increased in steps of 100 msec to several seconds (10-Hz laser repetition rate).

In order to photograph the image after several seconds of storage time, a Princeton Applied Research optical multi-channel analyzer (OMA) is used to store the image produced by the stimulated echo in its reticon array. The image stored by the OMA is subsequently displayed on an oscilloscope and photographed with a camera. Figure 4 shows the stimulated echo image recorded by the OMA with a first- to third-pulse separation of 3 sec. The image shown in Fig. 4 is produced by a mask of the same size as the one shown in Fig. 3. As can be seen from Fig. 4, the image is quite sharp and well defined. Furthermore, in this manner we have observed the spatial echo image to last for at least 15 sec.

Although we have not systematically measured the echo intensities as a function of  $t_{31}$ , we have observed that at  $t_{31} \approx 3$  sec the echo intensity is reduced by a factor of  $5 \times 10^3$  from its value at  $t_{31} = 97$  nsec. In addition, the image storage time is strongly dependent on the sample temperature. Specifically, the storage time increases by an order of magnitude when the sample temperature is reduced from 4.2 to 2.0 K. The strong temperature dependence suggests that the spin-lattice relaxation is probably the limiting relaxation mechanism.<sup>18</sup>

In summary, we have observed spatial-image storage in a

$\text{Pr}^{3+}:\text{LaF}_3$  sample below 4.2 K lasting for at least 15 sec. In addition, we have demonstrated that the stimulated echo in a solid is a phase-conjugate replica of the first excitation pulse.

## ACKNOWLEDGMENT

This research is supported by Nippon Telegraph and Telephone Corporation.

## REFERENCES

1. R. Kachru, T. W. Mossberg, and S. R. Hartmann, *Opt. Commun.* **30**, 57 (1979).
2. T. Mossberg, A. Flusberg, R. Kachru, and S. R. Hartmann, *Phys. Rev. Lett.* **42**, 1665 (1979).
3. J. B. W. Morsink and D. A. Wiersma, *Chem. Phys. Lett.* **65**, 105 (1979).
4. T. W. Mossberg, *Opt. Lett.* **7**, 77 (1982).
5. M. D. Levenson, *IBM Tech. Discl. Bull.* **24**, 2797 (1981).
6. N. S. Shiren, *Appl. Phys. Lett.* **33**, 299 (1978).
7. M. Fujita, H. Nakatsuka, H. Nakanishi, and M. Matsuoka, *Phys. Rev. Lett.* **42**, 974 (1979).
8. T. Kohmoto, H. Nakatsuka, and M. Matsuoka, *Jpn. J. Appl. Phys.* **22**, L571 (1983).
9. For a review of the phase-conjugate properties of optical echoes, see John C. AuYeung, in *Optical Phase Conjugation*, R. A. Fisher, ed. (Academic, New York, 1983), pp. 285-305.
10. N. W. Carlson, W. R. Babbitt, and T. W. Mossberg, *Opt. Lett.* **8**, 623 (1983).
11. P. Saari, R. Kaarli, and A. Rebane, *J. Opt. Soc. Am. B* **3**, 527 (1986); A. Rebane, R. Kaarli, P. Saari, A. Anijalg, and K. Timpmann, *Opt. Commun.* **47**, 173 (1983).
12. T. W. Mossberg, R. Kachru, S. R. Hartmann, and A. M. Flusberg, *Phys. Rev. A* **20**, 1976 (1979).
13. J. B. W. Morsink, W. H. Hesselink, and D. A. Wiersma, *Chem. Phys. Lett.* **64**, 1 (1979).
14. Y. C. Chen, K. P. Chiang, and S. R. Hartmann, *Opt. Commun.* **29**, 181 (1979).
15. L. E. Erickson, *Opt. Commun.* **21**, 147 (1977).
16. R. M. Shelby, C. S. Yannoni, and R. M. MacFarlane, *Phys. Rev. Lett.* **41**, 1739 (1978).
17. M. J. Weber, *J. Chem. Phys.* **48**, 4774 (1968).
18. R. M. Shelby, R. M. McFarlane, and C. S. Yannoni, *Phys. Rev. B* **21**, 5004 (1980).